Enhanced Ultraviolet Avalanche Photodiode With 640-nm-Thin Silicon Body Based on SOI Technology

Iman Sabri Alirezaei, Nicolas Andre, *Member, IEEE*, and Denis Flandre, *Senior Member, IEEE*

***Abstract*— We present a novel ultrathin avalanche photodiode (APD) with a silicon (Si) body thickness of 640 nm and optimized doping profiles to significantly improve the detection efficiency in ultraviolet (UV) spectral range from near UV (NUV) to UV-C (here studied down to 275 nm). The square photodiode is fabricated on silicon-on-insulator (SOI) substrate with an active area of 420 μm^2 (37 $\mu m \times 37\ \mu m$) consisting of n^{++}/p-well and an n-well guard ring (GR). The dark current–voltage (*I–V*) characteristic exhibits low leakage current ($\approx$pA) and breakdown voltage of 8.6 V. A peak quantum efficiency (QE) of 93.88% is obtained on a wavelength of 400 nm at 4 V. An outstanding expansion of the sensitivity in UV-C is presented with a QE of 82.75% under a wavelength of 275 nm at 4 V. With a gain value of 4.9, a responsivity of 14.46 A/W at a wavelength of 400 nm on a low-level light intensity of 3.28 $\mu W/cm^2$ is achieved at 7.8 V. A sufficient detection performance in visible spectral range has also been achieved due to the formation of the sandwiched thin silicon body between nearly 200-nm SiO_2 on top and 1-μm buried SiO_2 (BOX). This proposed ultrathin photodiode indicates a potential high avalanche gain ($>10^5$) in Geiger mode.**

***Index Terms*— Avalanche photodiode (APD), low-light level, silicon-on-insulator (SOI) CMOS technology, ultraviolet (UV)-APD.**

I. Introduction

ULTRAVIOLET-ENHANCED avalanche photodiodes (APDs) operating on low light detection are of great interest in fluorescence lifetime imaging microscopy [1], time-of-flight (TOF) ultraviolet (UV) spectroscopy, positron emission tomography (PET) scanners for diagnostics and medical monitoring [2], fluorescence resonance energy transfer (FRET) (~250–470 nm), and many other biological identification systems [3], [4].

The UV detection efficiency in silicon-based detectors suffers from a very shallow absorption depth (less than 100 nm in the UV regime below 400 nm). Therefore, to increase the detection efficiency, it requires to exploit an ultrashallow junction with a proper space charge region width, still providing acceptable leakage current, breakdown voltage, and avalanche gain. The methods that have already been reported to realize an optimum ultrashallow junction are based, notably on the formation of p^+-n junction by the implantation of pure boron (PureB), for the spectral range from 2 to 400 nm [5], [6], and the epitaxial growth of thin p^+ doped silicon layer consisting of a steep doping gradient on a n-type silicon [7], or the epitaxial growth of ultrashallow boron gradient doping epitaxial layer in p^+-i-n APD [8]. The latter APD was studied in the wavelength range from 200 to 300 nm and demonstrated an avalanche gain of 2800 at a reverse bias voltage of 10.8 V and with a nanoampere dark current.

Using boron gradient doping profile instead of constant doping profile was exploited to obtain a strong electric field close to the surface (with a maximum value of 5.88×10^4 V/cm), resulting in a higher collection efficiency of photogenerated carriers and a higher responsivity of ~0.055 to ~0.11 A/W at 300 nm wavelength, depending on the doping time under the temperature at 900 °C [8].

In this article, we introduce a new ultrathin APD with a silicon body thickness of 640 nm based on silicon-on-insulator (SOI) technology. This photodiode consists of a gradient p-well doping profile to form a strong built-in electric field at shallow n^{++}/p-junction within the multiplication region and n-well guard ring (GR) to prevent a premature edge breakdown. The strong electric field at junction ($\sim 7.93 \times 10^5$ V/cm) enhances the charge collection efficiency and avalanche gain. The ultrathin Si film with a shallow junction and an optimum electric field within the multiplication region enables a significant enhancement of the photoresponsivity in the UV spectral range. Besides, this thin structure can minimize the bulk leakage current, correlated noise, and secondary effects in avalanche process, which originate from bulk substrate. The optimization of doping profile and diode structure is carried out via the simulations of several processing steps of thermal SiO_2 growth, ion implantation and annealing in SILVACO (Athena), and figures of merit of the resulting APD using SILVACO (Atlas) simulation (Section II). In this article, we finally report and compare the experimental APD static performance to the state of the art (Section III).

Manuscript received June 15, 2020; revised August 5, 2020; accepted August 12, 2020. This work was supported by the CQIntégré Project funded by the Walloon Region, Belgium. The review of this article was arranged by Editor J. Huang. *(Corresponding author: Iman Sabri Alirezaei.)*

The authors are with ICTEAM, Université catholique de Louvain, 1348 Louvain-la-Neuve, Belgium (e-mail: iman.sabri@uclouvain.be).

Color versions of one or more of the figures in this article are available online at http://ieeexplore.ieee.org.

Digital Object Identifier 10.1109/TED.2020.3017699

TABLE I
PARAMETERS FOR ION IMPLANTATION DOPING PROCESS

Regions	Ion implantation process
p-well	Boron, Dose = 4×10^{13}cm^{-2}, Energy = 20 keV
p^{++}	Boron, Dose = 5×10^{15}cm^{-2}, Energy = 20 keV
n-well	Arsenic, Dose = 1.3×10^{13}cm^{-2}, Energy = 60 keV
n^{++}	Arsenic, Dose = 5×10^{15}cm^{-2}, Energy = 20 keV

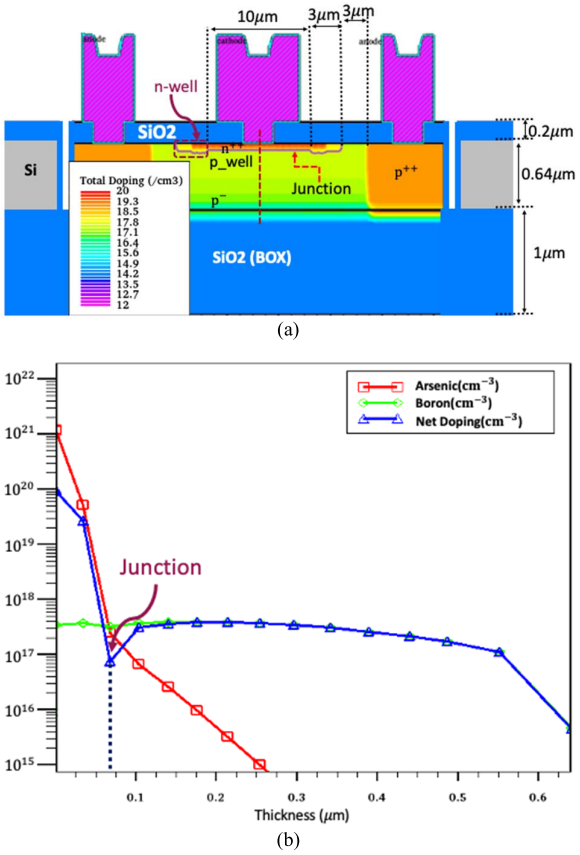

Fig. 1. (a) 2-D structure of the APD based on n^{++}/p-well and (b) simulated doping profile across the dashed line in the middle of the structure.

II. DEVICE STRUCTURE AND SIMULATION ANALYSIS

To enhance collection efficiency in UV, SOI technology is used to optimize the APD structure toward achieving excellent electrical performance under front-side light illumination. In a next step and future work, SOI will enable back-side illumination, with higher fill factor, after back-side bulk silicon (handle wafer) etching to buried oxide (BOX) while maintaining mechanical robustness and minimum stress of the thin membrane [12].

Wafer-level fabrication starts with a 700-nm-thick silicon layer and 1000-nm BOX. The final APD thickness is 640 nm after the four successive steps of ∼27-nm thermal oxidation, ion implantation, and subsequent SiO_2 etching, to construct the active device.

Fig. 1(a) shows the APD pixel structure with the final doping profile simulated by SILVACO (Athena) using the parameters of Table I. The doping gradient across the dashed line in the middle of 2-D-structure is shown in Fig. 1(b).

The 2-D cross section depicts a 13-μm avalanche region formed by the n^{++}/p-well junction. A 3-μm n-well GR with an overlap width of 1.5 μm on n^{++} region is also exploited around the avalanche region to avoid the premature edge breakdown. The doping level and the depth of the p-well play an important role to optimize the values of breakdown voltage and space charge region depth [9]. As shown in Fig. 2, a lower dose of boron-ion implantation (4×10^{13} cm^{-2}) for the p-well builds up a wider space charge region of 180 nm and a higher breakdown voltage.

The electric field profile at breakdown voltage is also shown in Fig. 2. A high built-in electric field of 7.93×10^5 V/cm is obtained in the multiplication region, which enhances the collection efficiency of photogenerated carriers [8].

Besides, this high electric field increases the impact ionization coefficients and the avalanche gain.

An optical microscope image of the fabricated square APD with a total pixel size of 37 μm × 37 μm is shown in Fig. 3. After the deposition of plasma enhanced chemical vapor deposition (PECVD)-SiO_2, the annealing process is done under oxygen at 700 °C to minimize the surface recombination rate in the interface of Si–SiO_2. Thereafter, Al (with 1% Si) is deposited for the contacts and metal interconnects. Furthermore, annealing is carried out in forming gas at 432 °C.

III. MEASUREMENT RESULTS AND DISCUSSION

Fig. 4 shows the measured I–V curves of the fabricated APD at room temperature for dark and under LED illumination at a wavelength of 386 nm on a low light intensity of 29 μW/cm^2, as well as the avalanche gain. The avalanche gain is given by the following equation [10]:

$$\text{Gain} = (I_{\text{Illuminated}} - I_{\text{Dark}})/(I_{\text{P-Illuminated}} - I_{\text{P-Dark}}) \quad (1)$$

where $I_{\text{Illuminated}}$ and I_{Dark} are the illuminated and dark currents, respectively. $I_{\text{P-Illuminated}}$ and $I_{\text{P-Dark}}$ denote the primary illuminated and the primary dark current at 0.05 V, respectively.

The proposed APD achieves a low dark current on the order of picoampere (pA) with a breakdown voltage of 8.6 V, which fairly fits the simulated result for a boron-ion implantation dose of 4×10^{13} cm^{-2} for the p-well. The gain achieves a very high value in the avalanche region ($>10^5$). This range of gain is well suited for exploiting the ultrathin APD integrated with a quench circuit in Geiger mode as a single photon avalanche detector (SPAD) for application in UV spectral range.

The photoresponsivity and the quantum efficiency (QE) below breakdown, at 4 V for Gain $\simeq$ 1, are shown in Fig. 5. A maximum QE of 93.88%, corresponding to a responsivity of 0.3 A/W, is obtained at a wavelength of 400 nm. Besides, the expansion of this photodiode sensitivity down to UV-C is remarkable, thanks to the formation of shallow junction, optimized space charge region depth, and implementation of ultrathin silicon film with a thickness of about 640 nm.

Therefore, QE of 82.75% and responsivity of 0.18 A/W are achieved at a wavelength of 275 nm. To the best of authors' knowledge, this QE is the best result ever reported for a Si-based APD.

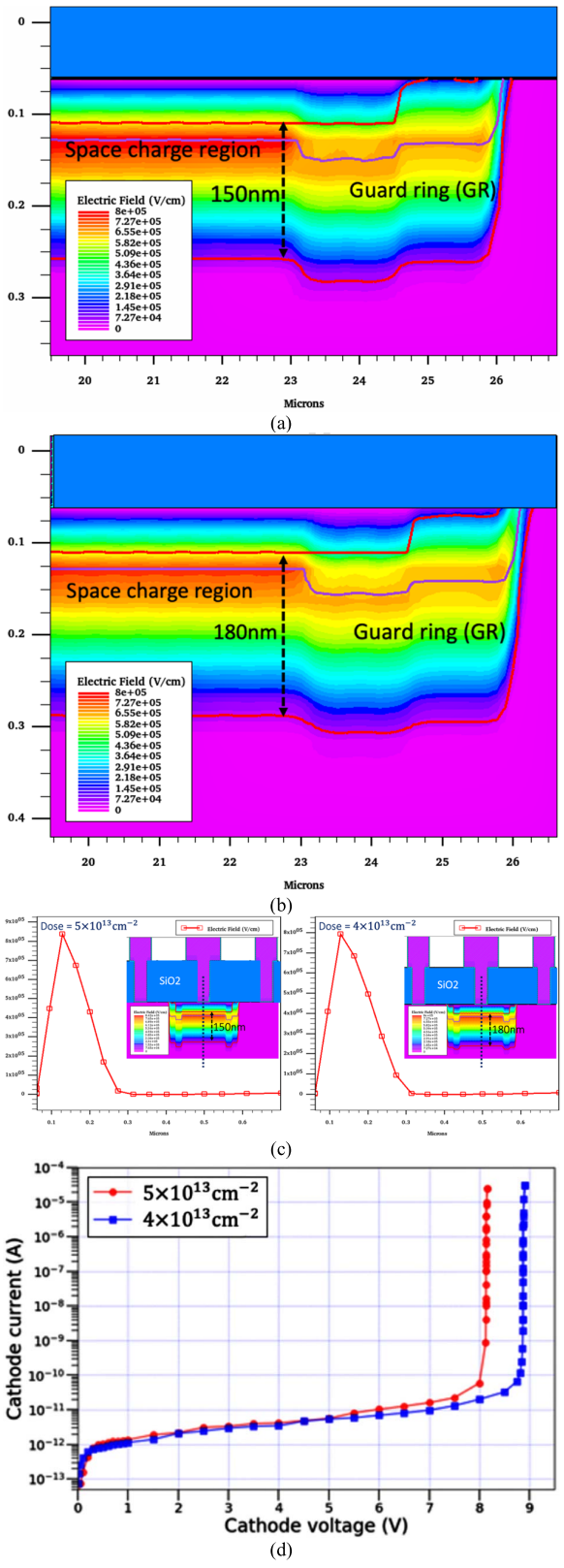

Fig. 2. Simulated electric field profile and the depth of space charge region (red line) at the breakdown voltage for (a) dose of 5×10^{13} cm^{-2} and (b) dose of 4×10^{13} cm^{-2} boron implantation in p-well with (c) 1-D electric field profile across the dashed line in the inset structure as well as (d) dark *I–V* curves for the respective implantation doses.

Fig. 6 shows the responsivity for two wavelengths of 386 and 400 nm as a function of reverse bias up to the linear avalanche mode, which is closely placed before the breakdown voltage. In this static voltage range, the responsivity enhancement follows the value of the gain. A responsivity of 14.46 A/W at 400 nm is then attained at a reverse bias of 7.8 V.

A further performance comparison of the presented SOI 640-nm-thick APD with the state of the art is shown in Table II, for comparable static bias conditions and light wavelength within the UV spectral region. The responsivity at 275 nm and Gain $\simeq$ 1 in the proposed APD at 4 V is

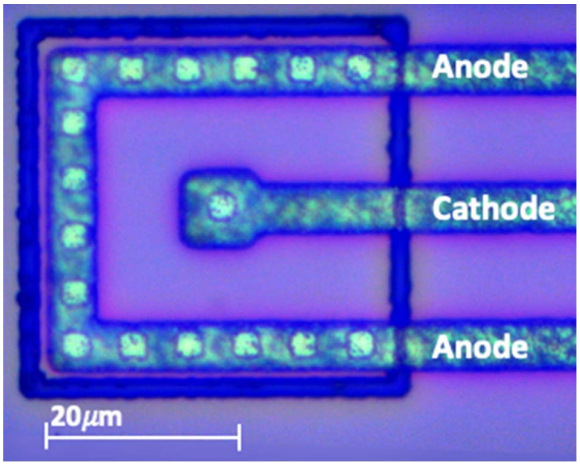

Fig. 3. An optical microscope image of the fabricated enhanced UV APD with 640-nm-thin silicon body.

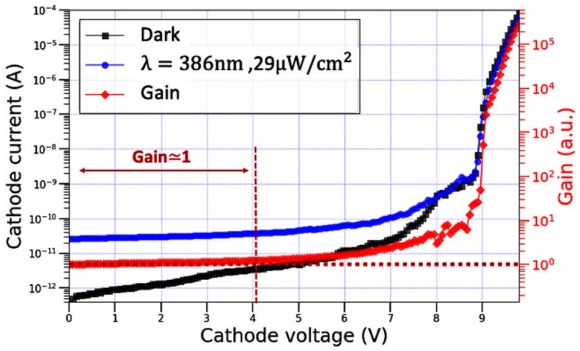

Fig. 4. Current–voltage (*I–V*) characteristic under dark and illumination at a wavelength of 386 nm with a low intensity of 29 μW/cm^2 and the calculated avalanche gain.

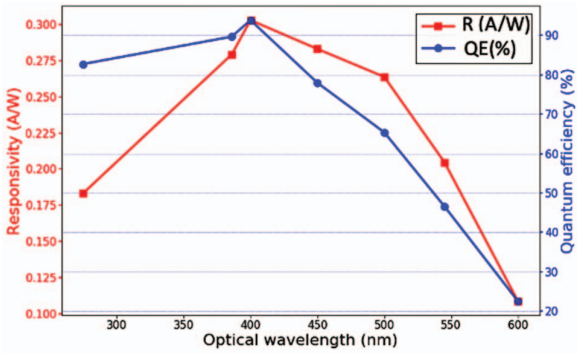

Fig. 5. Photoresponsivity and QE of the fabricated APD in the spectral range from 275 to 600 nm at 4-V reverse bias.

TABLE II
OVERVIEW ON THE STATIC PERFORMANCE OF SILICON-BASED AVALANCHE PHOTODETECTORS IN UV RANGE

	pn junction	Methods	V_{Br} (V)	Dark current	Responsivity (A/W)
[5, 6]	p^+/n	PureB	~14 (d =4μm) [a]	~ 10fA at 12.5V	~ 0.07 at λ =275nm
[8]	p^+-i-n	Epitaxial B gradient doping	10.6 (d=50μm) [a]	~ 1nA at 8V	~ 0.08 at λ =275nm
[7]	p^+/n	Epitaxial growth of p^+ doped Silicon	1600< ($1cm^2$)	~ Minimum: 30nA at 600V	~ Maximum: 0.14 at λ =350nm
[11]	p^+/n-well	0.8μm CMOS process	19.5($0.5mm^2$)	~ 70pA at 17.5V	~ 0.01 at λ =300nm
This work	n^{++}/p-well	**SOI process**	**8.6 (420μm²)**	**12pA at 6V**	**~0.18 at λ =275nm**

[a] d denotes the diameter of the junction in the circular detectors.

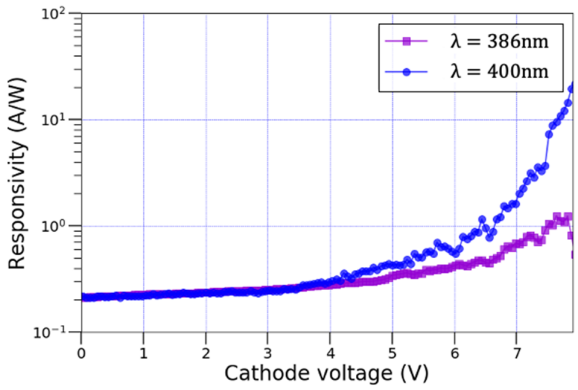

Fig. 6. Photoresponsivity versus reverse bias measured at two wavelengths of 386 and 400 nm.

2.25 times and 2.57 times higher than the reported detectors in [5], [6], and [8], respectively. The breakdown voltage in the detector is also interestingly lower than other comparable detectors.

IV. CONCLUSION

We demonstrated a new ultrathin APD based on SOI technology. It consists of an optimized n^{++}/gradient p-well realized on a 640-nm-thin silicon film. The proposed photodiode has shown a low dark current and an outstanding sensitivity under low light intensity in the UV spectral range with a peak responsivity of 0.3 A/W at 400 nm for 4-V reverse bias, where the gain is equal to 1. The responsivity of the proposed photodiode at a wavelength of 275 nm exceeds the state of art with 0.18 A/W (gain $\simeq$ 1) at 4 V. The built-in electric field and the depth of the space charge region have been optimized by modifying the doping level in the p-well. The simulated electric field exhibits an electric field of 7.93×10^5 V/cm at the breakdown voltage of 8.6 V. A high avalanche gain ($>10^5$) can also be achieved, further increasing the responsivity. Accordingly, the demonstrated APD can next be applied in Geiger mode as a UV-enhanced single SPAD.

REFERENCES

[1] J. L. Lagarto *et al.*, "Real-time multispectral fluorescence lifetime imaging using single photon avalanche diode arrays," *Sci. Rep.*, vol. 10, no. 1, p. 8116, Dec. 2020, doi: 10.1038/s41598-020-65218-3.
[2] V. C. Spanoudaki and C. S. Levin, "Photo-detectors for time of flight positron emission tomography (ToF-PET)," *Sensors*, vol. 10, no. 11, pp. 10484–10505, Nov. 2010, doi: 10.3390/s101110484.
[3] C. Bruschini, H. Homulle, I. M. Antolovic, S. Burri, and E. Charbon, "Single-photon avalanche diode imagers in biophotonics: Review and outlook," *Light, Sci. Appl.*, vol. 8, no. 1, p. 87, Dec. 2019, doi: 10.1038/s41377-019-0191-5.
[4] P. Sun, R. Ishihara, and E. Charbon, "Flexible ultrathin-body single-photon avalanche diode sensors and CMOS integration," *Opt. Express*, vol. 24, no. 4, pp. 3734–3748, 2016, doi: 10.1364/OE.24.003734.
[5] L. K. Nanver *et al.*, "Robust UV/VUV/EUV PureB photodiode detector technology with high CMOS compatibility," *IEEE J. Sel. Topics Quantum Electron.*, vol. 20, no. 6, pp. 306–316, Nov. 2014.
[6] L. Qi, K. R. C. Mok, E. Charbon, L. K. Nanver, M. Aminian, and E. Charbon, "UV-sensitive low dark-count PureB single-photon avalanche diode," in *Proc. IEEE Sensors*, Nov. 2013, pp. 1–4.
[7] R. A. Myers, R. Farrell, S. L. Riccardi, and M. McClish, "UV-enhanced silicon avalanche photodiodes," *Proc. SPIE*, vol. 8621, Mar. 2013, Art. no. 86211H, doi: 10.1117/12.2003993.
[8] Z. Xia *et al.*, "High-sensitivity silicon ultraviolet p+-i-n avalanche photodiode using ultra-shallow boron gradient doping," *Appl. Phys. Lett.*, vol. 111, no. 8, Aug. 2017, Art. no. 081109, doi: 10.1063/1.4985591.
[9] M.-J. Lee *et al.*, "High-performance back-illuminated three-dimensional stacked single-photon avalanche diode implemented in 45-nm CMOS technology," *IEEE J. Sel. Topics Quantum Electron.*, vol. 24, no. 6, pp. 1–9, Nov. 2018.
[10] A. Goushcha and B. Tabbert, "Optical detectors BT," in *Springer Handbook of Lasers and Optics*, F. Träger, Ed. New York, NY, USA: Springer, 2007, pp. 503–562.
[11] A. Rochas, A. R. Pauchard, P.-A. Besse, D. Pantic, Z. Prijic, and R. S. Popovic, "Low-noise silicon avalanche photodiodes fabricated in conventional CMOS technologies," *IEEE Trans. Electron Devices*, vol. 49, no. 3, pp. 387–394, Mar. 2002, doi: 10.1109/16.987107.
[12] M.-J. Lee, P. Sun, and E. Charbon, "A first single-photon avalanche diode fabricated in standard SOI CMOS technology with a full characterization of the device," *Opt. Express*, vol. 23, no. 10, pp. 13200–13209, 2015, doi: 10.1364/OE.23.013200.